Supplement of

Long-range transport biomass burning emissions to the Himalayas: insights from high-resolution aerosol mass spectrometry

Xinghua Zhang et al.

Correspondence to: Jianzhong Xu (jzxu@lzb.ac.cn)

Text

Text S1. Estimation of organic nitrates

Organic nitrates, which are produced either by photochemical (OH-initiated) or nocturnal (NO_3-initiated) oxidation reactions of anthropogenic and biogenic volatile organic compounds (VOCs), are important components of secondary organic aerosol in the troposphere (Farmer et al., 2010). Model studies have suggested that photochemical ON production accounts for a substantial fraction of SOA functionalization (Camredon et al., 2007).

The total nitrates measured by the HR-ToF-AMS is the nitrate functionality ($–ONO_2$), which may consist of both inorganic and organic nitrates. However, the direct measurements of particle-phase organic nitrates are not available currently with the HR-ToF-AMS measurements. For solving this restriction, an estimation method based on the NO^+/NO_2^+ ratio (denoted as NO_x^+ ratio method hereafter) in the AMS mass spectra is used widely to separate the measured total nitrates into nitrate functionality from inorganic and organic nitrates Farmer et al. (2010). Previous laboratory studies have shown that the NO_x^+ ratios are substantially different for organic nitrates and inorganic nitrate (NH_4NO_3), namely the ratios for organic nitrates are typically 2–3 times higher than those for NH_4NO_3 (Fry et al., 2009; Bruns et al., 2010; Farmer et al., 2010; Boyd et al., 2015). Based on the difference in NO_x^+ ratios, Farmer et al. (2010) have proposed an estimation method to calculate the concentrations of NO^+ and NO_2^+ fragments from organic nitrate by the following equations.

$$\mathrm{NO}_{2,\mathrm{ON}} = \frac{\mathrm{NO}_{2,\mathrm{meas}} \times (R_{\mathrm{meas}} - R_{\mathrm{AN}})}{R_{\mathrm{ON}} - R_{\mathrm{AN}}} \tag{1}$$

$$\mathrm{NO}_{\mathrm{ON}} = R_{\mathrm{ON}} \times \mathrm{NO}_{2,\mathrm{ON}} \tag{2}$$

where the subscripts meas, AN, and ON are denoted as concentrations of NO^+ and NO_2^+ fragments or NO_x^+ ratios (R_{meas}, R_{AN} and R_{ON}) from ambient measurement, pure ammonium nitrate and organic nitrates, respectively.

In this study, the R_{AN} values were determined from ionization efficiency (IE) calibrations using ammonium nitrate particles at the beginning, the middle, and the end of the campaigns, with an average value of 3.08 ± 0.15, which was within the range reported in the literature. Although the R_{ON} value is more difficult to determine due to its variance between instruments and precursor volatile organic compounds, a $R_{\mathrm{ON}}/R_{\mathrm{AN}}$ ratio which has been revealed to be instrument independent was determined widely for different organic nitrates in the literature, with values ranging from 2.08 for isoprene to 3.99 for β-pinene (Bruns et al., 2010; Fry et al., 2013; Boyd et al., 2015). Thus, the lower and upper values of R_{ON} can be estimated by multiplying R_{AN} value determined from IE calibrations with $R_{\mathrm{ON}}/R_{\mathrm{AN}}$ mentioned above. Finally, the lower and upper limits of R_{ON} were calculated to be 6.41 and 12.29, respectively, to estimate the amount of organic nitrates in this study. Noting that this method is relatively rough to estimate the organic nitrates based on the HR-ToF-AMS data, the direct and accurate measurement of organic nitrates warrants further study.

Most of the measured ambient NO^{+}/NO_{2}^{+} ratios are within the range of the calibrated value (i.e., R_{AN}, 3.08) and the estimated upper value (i.e., $R_{ON,\ upper}$, 12.29) and with an average value of 4.43 ± 1.39, which make the estimation of organic nitrates at QOMS possible. The time series of the measured total nitrate concentrations and NO^{+}/NO_{2}^{+} ratios as well as the estimated lower and upper nitrate functionality from organic nitrates in this study are displayed in Fig. S8, while the diurnal cycle of mass concentration of the estimated organic nitrate is showed in Fig. S9. Finally, the average lower and upper nitrate functionality from organic nitrates are estimated to be 0.031 and 0.048 μg m^{-3}, respectively, which contributed 15–23 % of the total measured nitrate, suggesting that organic nitrates are significant components in aerosol particles at QOMS. This result is comparable with other studies based on AMS data. For example, Xu et al. (2015) has estimated that the nitrate functionality from organic nitrates could contribute about 63–100 and 10–20% of the total measured nitrates in summer and winter in the southeastern USA, respectively. Zhu et al. (2016) also estimated the nitrate functionality from organic nitrates in a southern China background site, which was calculated to be 15–22 % of the total measured nitrates.

Tables

Table S1. Summary of the average mass concentrations of total PM_1 and chemical compositions measured with the Aerodyne AMS instruments at various remote sites worldwide.

Dataset Location	PM_1	Organics	Sulfate	Nitrate	Ammonium	References
Mt. Jungfraujoch (3580 m a.s.l.), Switzerland	0.55	0.25	0.17	0.04	0.05	Fröhlich et al. (2015)
Mt. Jungfraujoch (3580 m a.s.l.), Switzerland	2.24	1.20	0.51	0.20	0.33	Zhang et al. (2007)
Mt. Whistler (2182 m a.s.l.), Canada	1.91	1.05	0.58	0.05	0.23	Sun et al. (2009)
Mt. Bachelor (2.8 km a.s.l.), USA	15.10					Zhou et al. (2017)
Mace Head, Ireland	1.53	0.50	0.75	0.05	0.23	Zhang et al. (2007)
Hyytiala, Finland	2.04	1.20	0.31	0.24	0.28	Zhang et al. (2007)
Storm Peak, USA	2.11	0.90	0.59	0.22	0.40	Zhang et al. (2007)
Duke Forest, USA	2.82	1.30	1.10	0.10	0.32	Zhang et al. (2007)
Chebogue, Canada	2.91	1.60	0.89	0.08	0.34	Zhang et al. (2007)
Okinawa Island, Japan	7.89	1.70	4.70	0.15	1.30	Jimenez et al. (2009)
Fukue Island, Japan	12.03	5.03	4.80	0.56	1.57	Takami et al. (2005)
Jeju Island, Korea	10.66	4.30	3.90	0.76	1.70	Jimenez et al. (2009)

Table S2. Coefficient of determination (R^2) between time series of OA factors and other aerosol species. Values indicating the three stronger correlations for each components are in bold.

R^2	BBOA	NOA	MO-OOA	BBOA + NOA	NOA + MO-OOA
Sulfate	0.39	0.46	0.65	0.48	0.70
Nitrate	**0.75**	0.51	0.64	**0.82**	0.72
Ammonium	0.68	**0.54**	**0.70**	0.78	**0.78**
Chloride	0.62	0.46	0.40	0.70	0.51
Sulfate + Nitrate	0.58	0.52	**0.70**	0.67	**0.77**
Sulfate + Nitrate + Chloride	0.59	0.53	**0.70**	0.68	**0.77**
BC	0.72	**0.57**	0.66	0.82	0.76
$C_2H_4O_2^+$	**0.91**	0.48	0.48	**0.96**	0.59
$C_3H_5O_2^+$	**0.87**	0.52	0.56	**0.94**	0.67
Organic nitrates	0.45	**0.62**	0.40	0.58	0.57

Figures

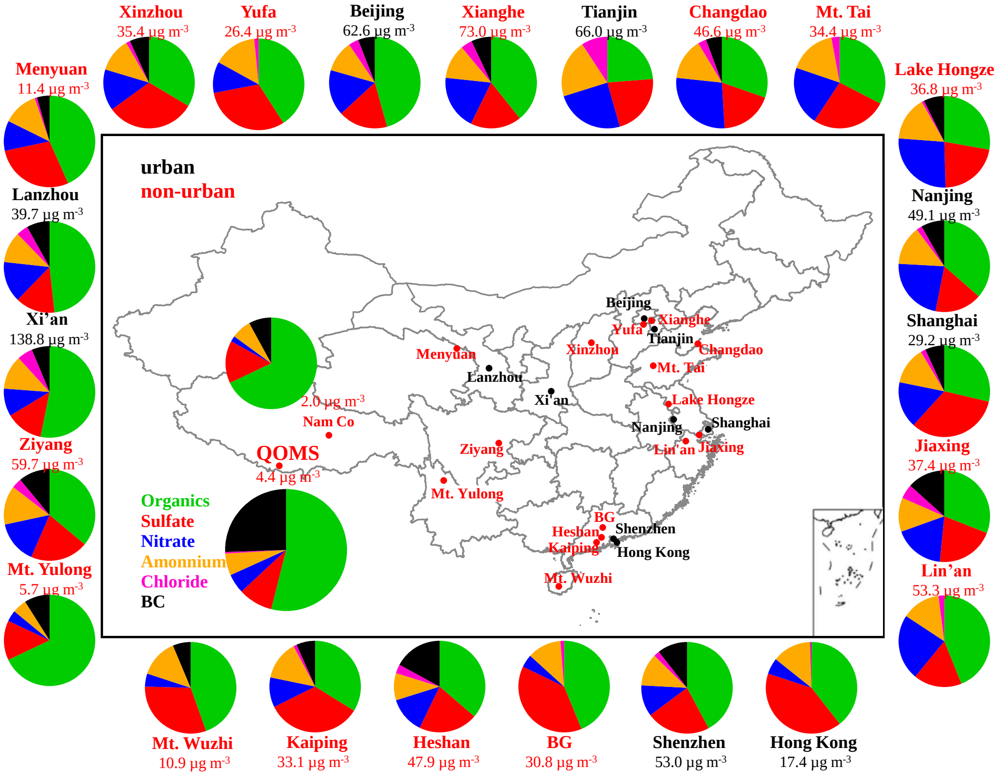

Fig. S1. Summary of the average mass concentrations and chemical compositions of PM$_1$ measured with the Aerodyne AMS and ACSM instruments at various sites in China. Colors for the site lables indicate the type of sampling location as urban (black) or non-urban (red) site. Colors for the each piechart represents chemical compositions as organics (green), sulfate (red), nitrate (blue), ammonium (orange), chloride (purple), and black carbon (black). Detailed data for each site can refer to studies conducted in Beijing (Huang et al., 2010; Sun et al., 2010; Sun et al., 2012; Jiang et al., 2013; Sun et al., 2013; Sun et al., 2014; Zhang et al., 2014a; Chen et al., 2015; Sun et al., 2015; Sun et al., 2016b), Tianjin (Zhang et al., 2012), Xi'an (Wang et al., 2014), Lanzhou (Xu et al., 2014; Xu et al., 2016; Zhang et al., 2017), Nanjing (Tang et al., 2014; Zhang et al., 2015b; Wang et al., 2016a), Shanghai (Huang et al., 2012), Shenzhen (Yao et al., 2010; He et al., 2011), Hong Kong (Li et al., 2015; Sun et al., 2016a), Yufa (Gunthe et al., 2011), Xianghe (Sun et al., 2016c), Xinzhou (Wang et al., 2016b), Changdao (Hu et al., 2013), Mt. Tai (Zhang et al., 2014b), Lake Hongze (Zhu et al., 2016), Jiaxing (Huang et al., 2013), Lin'an (Zhang et al., 2015a; Zhang et al., 2015c), Menyuan (Du et al., 2015), Ziyang (Hu et al., 2016), Mt. Yulong (Zheng et al., 2017), BG (Xiao et al., 2011), Heshan (Gong et al., 2012), Kaiping (Huang et al., 2011), Mt. Wuzhi (Zhu et al., 2016), Nam Co (Xu et al., 2017), and QOMS in this study, respectively.

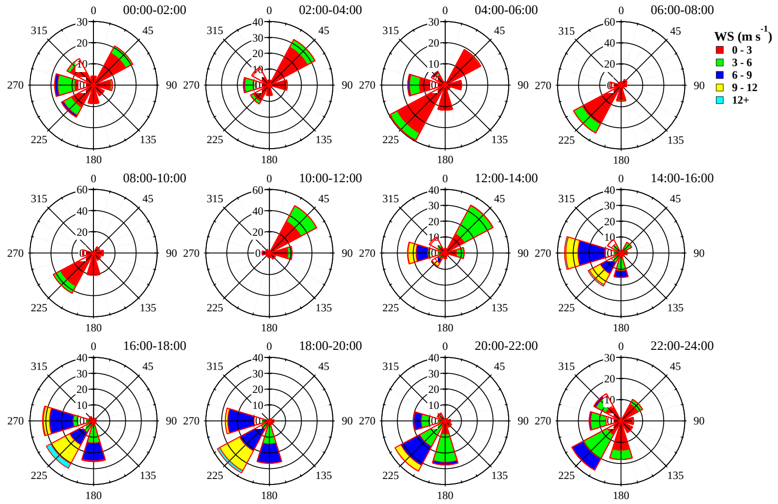

Fig. S2. Two-hour internal average wind rose plots for the entire period of 2016 Everest study.

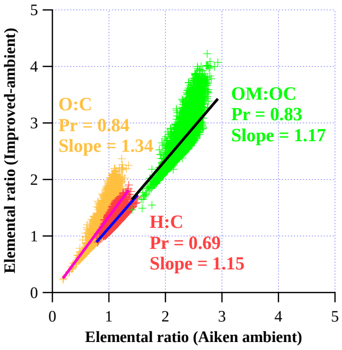

Fig. S3. Scatter plot of values calculated with "Improved-ambient" method versus that with "Aiken ambient" method

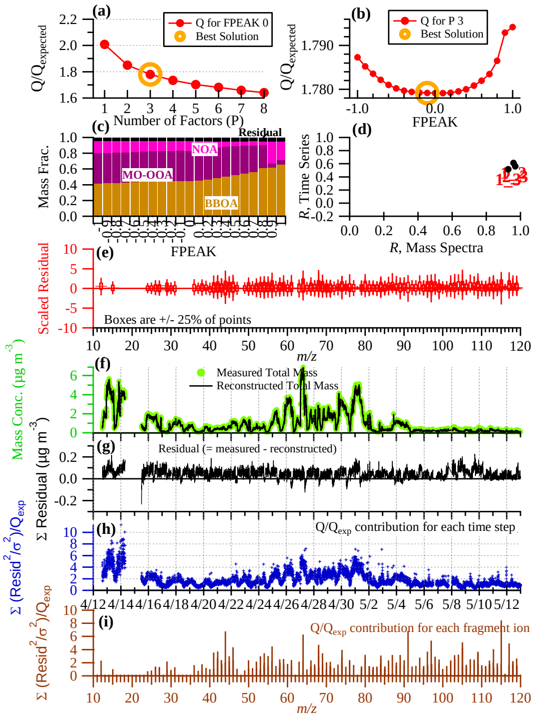

Fig. S4. Summary of key diagnostic plots of the PMF results: **(a)** Q/Q_{exp} as a function of number of factors (p) selected for PMF analysis. For the best solution (three factors solution): **(b)** Q/Q_{exp} as a function of FPEAK, **(c)** fractions of OA factors vs. FPEAK, **(d)** correlations among PMF factors, **(e)** the box and whiskers plot showing the distributions of scaled residuals for each m/z, **(f)** time series of the measured organic mass and the reconstructed organic mass (BBOA + Local-OOA + LRT-OOA), **(g)** variations of the residual (= measured - reconstructed) of the fit, **(h)** the Q/Q_{exp} for each point in time, and **(i)** the Q/Q_{exp} values for each ion.

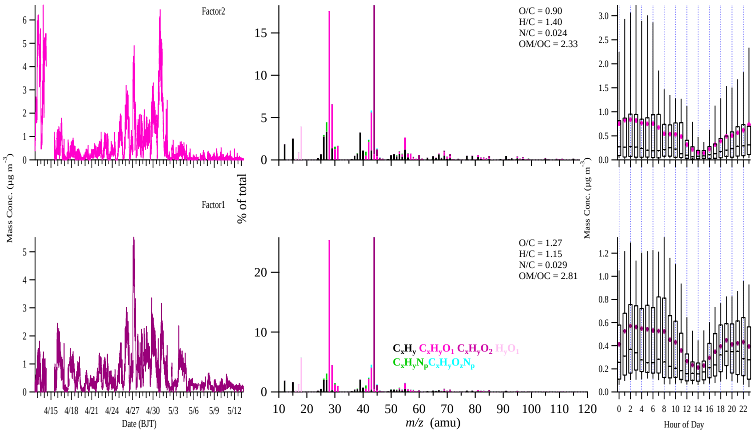

Fig. S5. Two factors solution analyzed by PMF analysis.

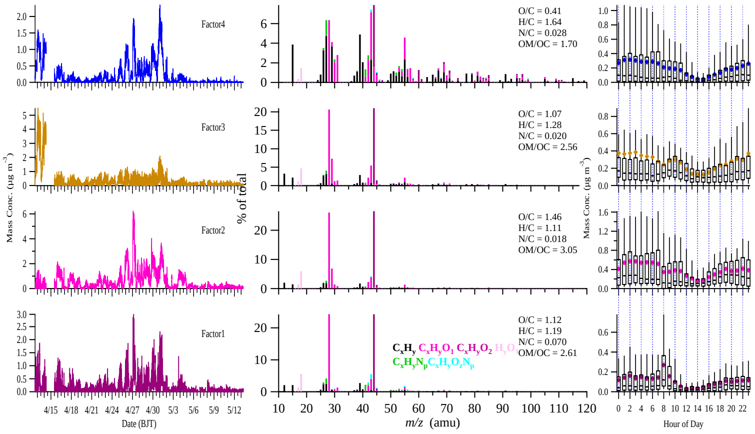

Fig. S6. Four factors solution analyzed by PMF analysis.

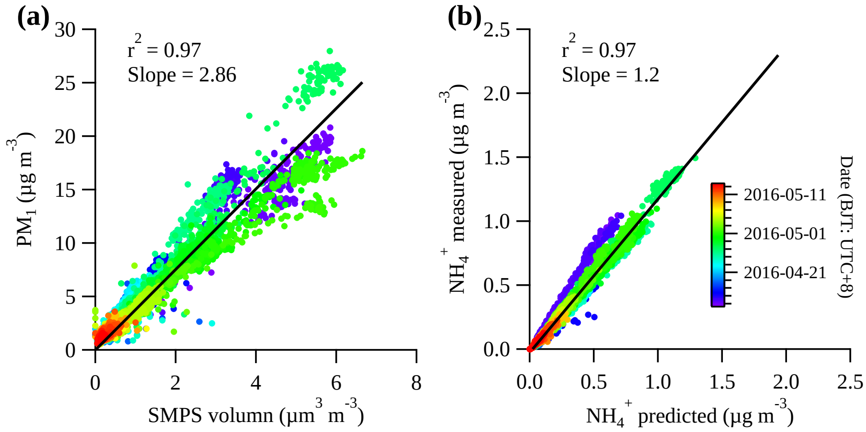

Fig. S7. Scatterplot of **(a)** PM_1 mass concentrations (NR-PM_1 + BC) versus particle volumes calculated from the SMPS by assuming spherical particles and **(b)** mass concentrations of measured NH_4^+ versus predicted NH_4^+. The predicted NH_4^+ concentrations were calculated based on the SO_4^{2-}, NO_3^-, and Cl^- concentrations from the AMS and assumed full neutralization of these anions by NH_4^+. Both the two black solid lines indicate the linear regression lines.

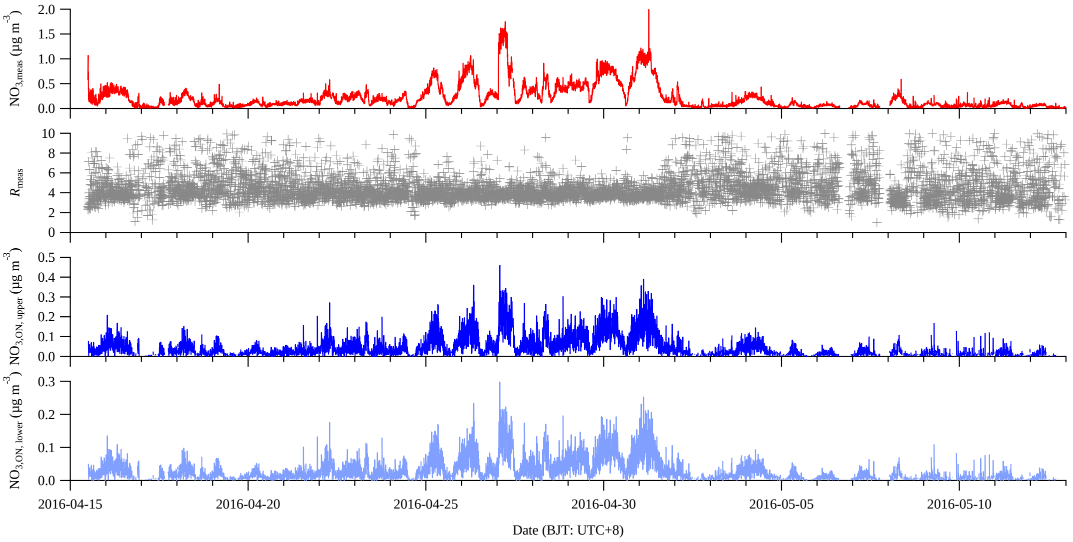

Fig. S8. The time series of the measured total nitrate concentrations and NO^+/NO_2^+ ratios as well as the estimated lower and upper organic nitrates.

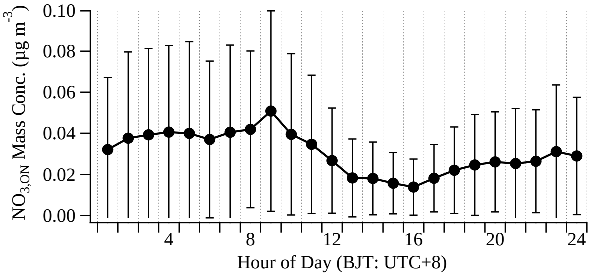

Fig. S9. The diurnal cycles of the estimated organic nitrates.

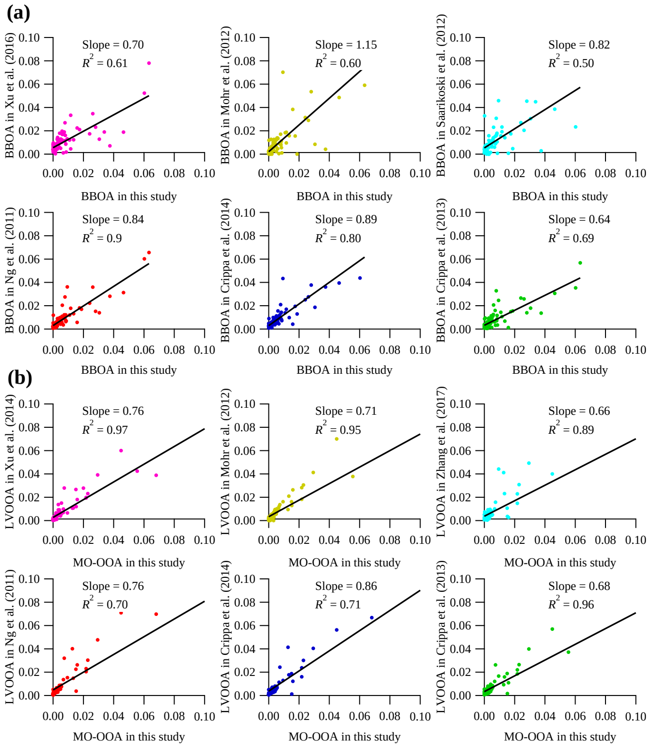

Fig. S10. Scatter plots of the high-resolution mass spectrums of BBOA (ignoring high signals on *m*/*z* 28 and 44) and MO-OOA in this study with those mass spectrums determined from other studies.

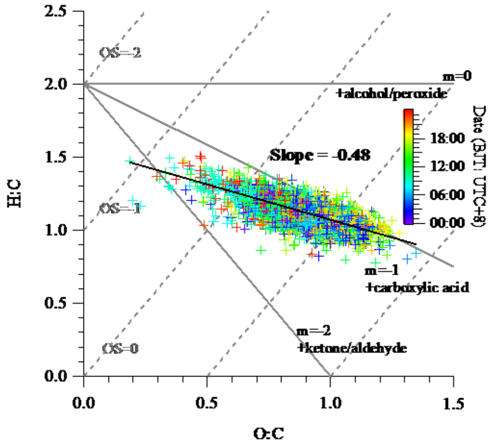

Fig. S11. Van Krevelen diagram for OA with linear fit. The measured OA data points are colored by time of the day.

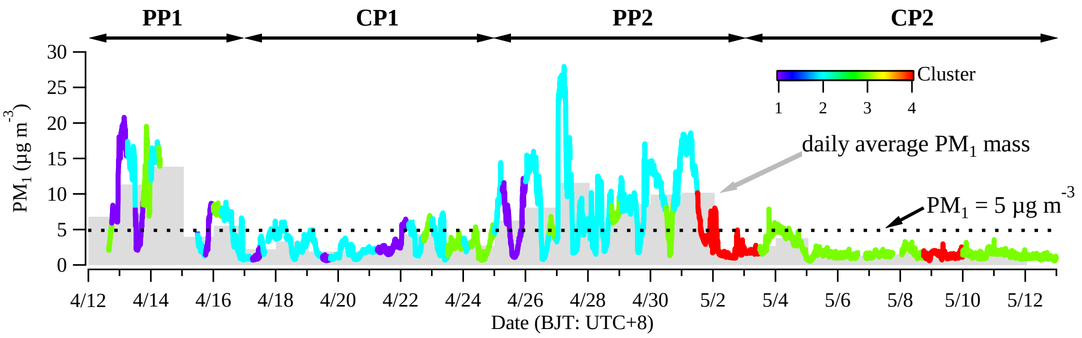

Fig. S12. Time series of 5-min PM_1 mass concentrations colored by different back trajectory clusters (line) and daily average PM_1 mass concentrations (grey histogram) for the entire study. The broken line indicate PM_1 mass concentrations equal to 5 μg m^{-3}. PP1 and PP2 are identified as two polluted periods while CP1 and CP2 are clear periods.

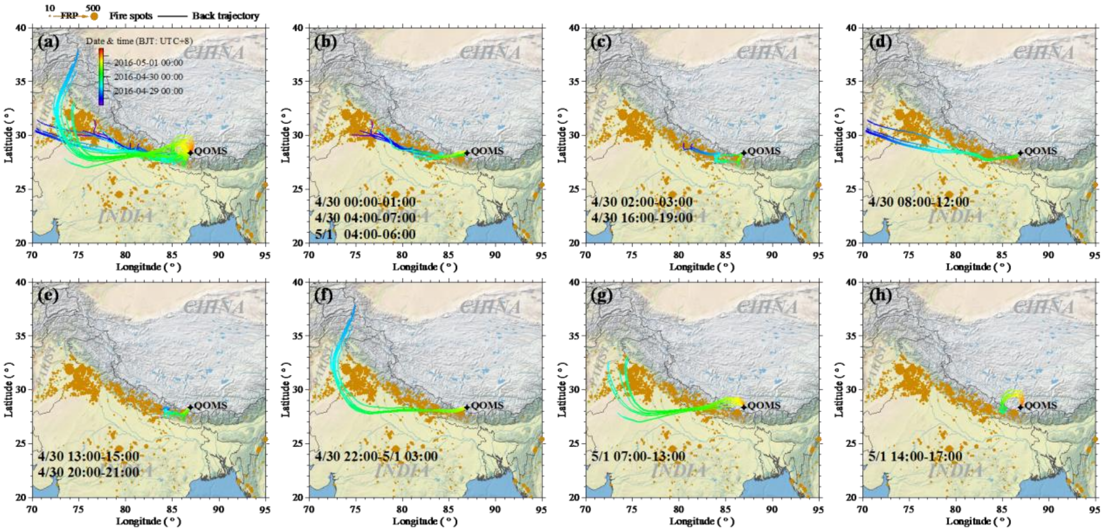

Fig. S13. The 48-h back trajectories calculated every 1 h and MODIS fire hotspots information for **(a)** the entire case study period from 30 April at 00:00 to 1 May at 18:00, and **(b-h)** different clusters during various time periods which have been marked in each figures.

References

Boyd, C. M., Sanchez, J., Xu, L., Eugene, A. J., Nah, T., Tuet, W. Y., Guzman, M. I., and Ng, N. L.: Secondary Organic Aerosol (SOA) formation from the β-pinene + NO3 system: effect of humidity and peroxy radical fate, Atmospheric Chemistry and Physics Discussions, 15, 2679-2744, doi:10.5194/acpd-15-2679-2015, 2015.

Bruns, E. A., Perraud, V., Zelenyuk, A., Ezell, M. J., Johnson, S. N., Yu, Y., Imre, D., Finlayson-Pitts, B. J., and Alexander, M. L.: Comparison of FTIR and Particle Mass Spectrometry for the Measurement of Particulate Organic Nitrates, Environ. Sci. Technol., 44, 1056-1061, doi:10.1021/es9029864, 2010.

Camredon, M., Aumont, B., Lee-Taylor, J., and Madronich, S.: The SOA/VOC/NOx system: an explicit model of secondary organic aerosol formation, Atmos. Chem. Phys., 7, 5599-5610, doi:10.5194/acp-7-5599-2007, 2007.

Chen, C., Sun, Y. L., Xu, W. Q., Du, W., Zhou, L. B., Han, T. T., Wang, Q. Q., Fu, P. Q., Wang, Z. F., Gao, Z. Q., Zhang, Q., and Worsnop, D. R.: Characteristics and sources of submicron aerosols above the urban canopy (260 m) in Beijing, China, during the 2014 APEC summit, Atmos. Chem. Phys., 15, 12879-12895, doi:10.5194/acp-15-12879-2015, 2015.

Du, W., Sun, Y. L., Xu, Y. S., Jiang, Q., Wang, Q. Q., Yang, W., Wang, F., Bai, Z. P., Zhao, X. D., and Yang, Y. C.: Chemical characterization of submicron aerosol and particle growth events at a national background site (3295 m a.s.l.) on the Tibetan Plateau, Atmos. Chem. Phys., 15, 10811-10824, doi:10.5194/acp-15-10811-2015, 2015.

Farmer, D. K., Matsunaga, A., Docherty, K. S., Surratt, J. D., Seinfeld, J. H., Ziemann, P. J., and Jimenez, J. L.: Response of an aerosol mass spectrometer to organonitrates and organosulfates and implications for atmospheric chemistry, Proc Natl Acad Sci U S A, 107, 6670-6675, doi:10.1073/pnas.0912340107, 2010.

Fröhlich, R., Cubison, M. J., Slowik, J. G., Bukowiecki, N., Canonaco, F., Croteau, P. L., Gysel, M., Henne, S., Herrmann, E., Jayne, J. T., Steinbacher, M., Worsnop, D. R., Baltensperger, U., and Prévôt, A. S. H.: Fourteen months of on-line measurements of the non-refractory submicron aerosol at the Jungfraujoch (3580 m a.s.l.) – chemical composition, origins and organic aerosol sources, Atmos. Chem. Phys., 15, 11373-11398, doi:10.5194/acp-15-11373-2015, 2015.

Fry, J. L., Kiendler-Scharr, A., Rollins, A. W., Wooldridge, P. J., Brown, S. S., Fuchs, H., Dubé, W., Mensah, A., dal Maso, M., Tillmann, R., Dorn, H. P., Brauers, T., and Cohen, R. C.: Organic nitrate and secondary organic aerosol yield from NO3 oxidation of β-pinene evaluated using a gas-phase kinetics/aerosol partitioning model, Atmos. Chem. Phys., 9, 1431-1449, doi:10.5194/acp-9-1431-2009, 2009.

Fry, J. L., Draper, D. C., Zarzana, K. J., Campuzano-Jost, P., Day, D. A., Jimenez, J. L., Brown, S. S., Cohen, R. C., Kaser, L., Hansel, A., Cappellin, L., Karl, T., Hodzic Roux, A., Turnipseed, A., Cantrell, C., Lefer, B. L., and Grossberg, N.: Observations of gas- and aerosol-phase organic nitrates at BEACHON-RoMBAS 2011, Atmos. Chem. Phys., 13, 8585-8605, doi:10.5194/acp-13-8585-2013, 2013.

Gong, Z., Lan, Z., Xue, L., Zeng, L., He, L., and Huang, X.: Characterization of submicron aerosols in the urban outflow of the central Pearl River Delta region of China, Front. Environ. Sci. Eng., 6, 725-733, doi:10.1007/s11783-012-0441-8, 2012.

Gunthe, S. S., Rose, D., Su, H., Garland, R. M., Achtert, P., Nowak, A., Wiedensohler, A., Kuwata, M., Takegawa, N., Kondo, Y., Hu, M., Shao, M., Zhu, T., Andreae, M. O., and Pöschl, U.: Cloud condensation nuclei (CCN) from fresh and aged air pollution in the megacity region of Beijing, Atmos. Chem. Phys., 11, 11023-11039, doi:10.5194/acp-11-11023-2011, 2011.

He, L. Y., Huang, X. F., Xue, L., Hu, M., Lin, Y., Zheng, J., Zhang, R., and Zhang, Y. H.: Submicron aerosol analysis and organic source apportionment in an urban atmosphere in Pearl River Delta of China using high-resolution aerosol mass spectrometry, J. Geophys. Res., 116, doi:10.1029/2010jd014566, 2011.

Hu, W., Hu, M., Hu, W.-W., Niu, H., Zheng, J., Wu, Y., Chen, W., Chen, C., Li, L., Shao, M., Xie, S., and Zhang, Y.: Characterization of submicron aerosols influenced by biomass burning at a site in the Sichuan Basin, southwestern China, Atmos. Chem. Phys., 16, 13213-13230, doi:10.5194/acp-16-13213-2016, 2016.

Hu, W. W., Hu, M., Yuan, B., Jimenez, J. L., Tang, Q., Peng, J. F., Hu, W., Shao, M., Wang, M., Zeng, L. M., Wu, Y. S., Gong, Z. H., Huang, X. F., and He, L. Y.: Insights on organic aerosol aging and the influence of coal combustion at a regional receptor site of central eastern China, Atmos. Chem. Phys., 13, 10095-10112, doi:10.5194/acp-13-10095-2013, 2013.

Huang, X.-F., Xue, L., Tian, X.-D., Shao, W.-W., Sun, T.-L., Gong, Z.-H., Ju, W.-W., Jiang, B., Hu, M., and He, L.-Y.: Highly time-resolved carbonaceous aerosol characterization in Yangtze River Delta of China: Composition, mixing state and secondary formation, Atmos. Environ., 64, 200-207, doi:10.1016/j.atmosenv.2012.09.059, 2013.

Huang, X. F., He, L. Y., Hu, M., Canagaratna, M. R., Sun, Y., Zhang, Q., Zhu, T., Xue, L., Zeng, L. W., Liu, X. G., Zhang, Y. H., Jayne, J. T., Ng, N. L., and Worsnop, D. R.: Highly time-resolved chemical characterization of atmospheric submicron particles during 2008 Beijing Olympic Games using an Aerodyne High-Resolution Aerosol Mass Spectrometer, Atmos. Chem. Phys., 10, 8933-8945, doi:10.5194/acp-10-8933-2010, 2010.

Huang, X. F., He, L. Y., Hu, M., Canagaratna, M. R., Kroll, J. H., Ng, N. L., Zhang, Y. H., Lin, Y., Xue, L., Sun, T. L., Liu, X. G., Shao, M., Jayne, J. T., and Worsnop, D. R.: Characterization of submicron aerosols at a rural site in Pearl River Delta of China using an Aerodyne High-Resolution Aerosol Mass Spectrometer, Atmos. Chem. Phys., 11, 1865-1877, doi:10.5194/acp-11-1865-2011, 2011.

Huang, X. F., He, L. Y., Xue, L., Sun, T. L., Zeng, L. W., Gong, Z. H., Hu, M., and Zhu, T.: Highly time-resolved chemical characterization of atmospheric fine particles during 2010 Shanghai World Expo, Atmos. Chem. Phys., 12, 4897-4907, doi:10.5194/acp-12-4897-2012, 2012.

Jiang, Q., Sun, Y. L., Wang, Z. F., and Yin, Y.: Real-time online measurements of the inorganic and organic composition of haze fine particles with an Aerosol Chemical Speciation Monitor (ACSM), Chin. Sci. Bull. (Chin Ver), 58, doi:10.1360/972013-501, 2013.

Jimenez, J. L., Canagaratna, M. R., Donahue, N. M., Prevot, A. S., Zhang, Q., Kroll, J. H., DeCarlo, P. F., Allan, J. D., Coe, H., Ng, N. L., Aiken, A. C., Docherty, K. S., Ulbrich, I. M., Grieshop, A. P., Robinson, A. L., Duplissy, J., Smith, J. D., Wilson, K. R., Lanz, V. A., Hueglin, C., Sun, Y. L., Tian, J., Laaksonen, A., Raatikainen, T., Rautiainen, J., Vaattovaara, P., Ehn, M., Kulmala, M., Tomlinson, J. M., Collins, D. R., Cubison, M. J., Dunlea, E. J., Huffman, J. A., Onasch, T. B., Alfarra, M. R., Williams, P. I., Bower, K., Kondo, Y., Schneider, J., Drewnick, F., Borrmann, S., Weimer, S., Demerjian, K., Salcedo, D., Cottrell, L., Griffin, R., Takami, A., Miyoshi, T., Hatakeyama, S., Shimono, A., Sun, J. Y., Zhang, Y. M., Dzepina, K., Kimmel, J. R., Sueper, D., Jayne, J. T., Herndon, S. C., Trimborn, A. M., Williams, L. R., Wood, E. C., Middlebrook, A. M., Kolb, C. E., Baltensperger, U., and Worsnop, D. R.: Evolution of organic aerosols in the atmosphere, Science, 326, 1525-1529, doi:10.1126/science.1180353, 2009.

Li, Y. J., Lee, B. P., Su, L., Fung, J. C. H., and Chan, C. K.: Seasonal characteristics of fine particulate matter (PM) based on high-resolution time-of-flight aerosol mass spectrometric (HR-ToF-AMS) measurements at the HKUST Supersite in Hong Kong, Atmos. Chem. Phys., 15, 37-53, doi:10.5194/acp-15-37-2015, 2015.

Sun, C., Lee, B. P., Huang, D., Jie Li, Y., Schurman, M. I., Louie, P. K. K., Luk, C., and Chan, C. K.: Continuous measurements at the urban roadside in an Asian megacity by Aerosol Chemical Speciation Monitor (ACSM): particulate matter characteristics during fall and winter seasons in Hong Kong, Atmos. Chem. Phys., 16, 1713-1728, doi:10.5194/acp-16-1713-2016, 2016a.

Sun, J. Y., Zhang, Q., Canagaratna, M. R., Zhang, Y. M., Ng, N. L., Sun, Y. L., Jayne, J. T., Zhang, X. C., Zhang, X. Y., and Worsnop, D. R.: Highly time- and size-resolved characterization of submicron aerosol particles in Beijing using an Aerodyne Aerosol Mass Spectrometer, Atmos. Environ., 44, 131-140, doi:10.1016/j.atmosenv.2009.03.020, 2010.

Sun, Y., Zhang, Q., Macdonald, A., Hayden, K., Li, S., Liggio, J., Liu, P., Anlauf, K., Leaitch, W., and Steffen, A.: Size-resolved aerosol chemistry on Whistler Mountain, Canada with a high-resolution aerosol mass spectrometer during INTEX-B, Atmos. Chem. Phys., 9, 3095-3111, doi:10.5194/acp-9-3095-2009, 2009.

Sun, Y., Jiang, Q., Wang, Z., Fu, P., Li, J., Yang, T., and Yin, Y.: Investigation of the sources and evolution processes of severe haze pollution in Beijing in January 2013, J. Geophys. Res. Atmos., 119, 4380-4398, 2014.

Sun, Y., Du, W., Wang, Q., Zhang, Q., Chen, C., Chen, Y., Chen, Z., Fu, P., Wang, Z., Gao, Z., and Worsnop, D. R.: Real-Time Characterization of Aerosol Particle Composition above the Urban Canopy in Beijing: Insights into the Interactions between the Atmospheric Boundary Layer and Aerosol Chemistry, Environ. Sci. Technol., 49, 11340-11347, doi:10.1021/acs.est.5b02373, 2015.

Sun, Y., Du, W., Fu, P., Wang, Q., Li, J., Ge, X., Zhang, Q., Zhu, C., Ren, L., Xu, W., Zhao, J., Han, T., Worsnop, D. R., and Wang, Z.: Primary and secondary aerosols in Beijing in winter: sources, variations and processes, Atmos. Chem. Phys., 16, 8309-8329, doi:10.5194/acp-16-8309-2016, 2016b.

Sun, Y., Jiang, Q., Xu, Y., Ma, Y., Zhang, Y., Liu, X., Li, W., Wang, F., Li, J., Wang, P., and Li, Z.: Aerosol characterization over the North China Plain: Haze life cycle and biomass burning impacts in summer, J. Geophys. Res. Atmos., 121, 2508-2521, doi:10.1002/2015jd024261, 2016c.

Sun, Y. L., Wang, Z. F., Dong, H. B., Yang, T., Li, J., Pan, X. L., Chen, P., and Jayne, J. T.: Characterization of summer organic and inorganic aerosols in Beijing, China with an Aerosol Chemical Speciation Monitor, Atmos. Environ., 51, 250-259, doi:10.1016/j.atmosenv.2012.01.013, 2012.

Sun, Y. L., Wang, Z. F., Fu, P. Q., Yang, T., Jiang, Q., Dong, H. B., Li, J., and Jia, J. J.: Aerosol composition, sources and processes during wintertime in Beijing, China, Atmos. Chem. Phys., 13, 4577-4592, doi:10.5194/acp-13-4577-2013, 2013.

Takami, A., Miyoshi, T., Shimono, A., and Hatakeyama, S.: Chemical composition of fine aerosol measured by AMS at Fukue Island, Japan during APEX period, Atmos. Environ., 39, 4913-4924, doi:10.1016/j.atmosenv.2005.04.038, 2005.

Tang, L., Zhang, Y., Sun, Y., Yu, H., Zhou, H., Wang, Z., Qin, W., Chen, P., Zhang, H., Chen, Y., and Jiang, R.: Components and optical properties of submicron aerosol during the lasting haze period in Nanjing, Chin. Sci. Bull. (Chin Ver), 59, 1955, doi:10.1360/972013-1098, 2014.

Wang, J., Ge, X., Chen, Y., Shen, Y., Zhang, Q., Sun, Y., Xu, J., Ge, S., Yu, H., and Chen, M.: Highly time-resolved urban aerosol characteristics during springtime in Yangtze River Delta, China: insights from soot particle aerosol mass spectrometry, Atmos. Chem. Phys., 16, 9109-9127, doi:10.5194/acp-16-9109-2016, 2016a.

Wang, Q., Huang, R. J., Cao, J., Han, Y., Wang, G., Li, G., Wang, Y., Dai, W., Zhang, R., and Zhou, Y.: Mixing State of Black Carbon Aerosol in a Heavily Polluted Urban Area of China: Implications for Light Absorption Enhancement, Aerosol Sci. Technol., 48, 689-697, doi:10.1080/02786826.2014.917758, 2014.

Wang, Q., Zhao, J., Du, W., Ana, G., Wang, Z., Sun, L., Wang, Y., Zhang, F., Li, Z., Ye, X., and Sun, Y.: Characterization of submicron aerosols at a suburban site in central China, Atmos. Environ., 131, 115-123, doi:10.1016/j.atmosenv.2016.01.054, 2016b.

Xiao, R., Takegawa, N., Zheng, M., Kondo, Y., Miyazaki, Y., Miyakawa, T., Hu, M., Shao, M., Zeng, L., Gong, Y., Lu, K., Deng, Z., Zhao, Y., and Zhang, Y. H.: Characterization and source apportionment of submicron aerosol with aerosol mass spectrometer during the PRIDE-PRD 2006 campaign, Atmos. Chem. Phys., 11, 6911-6929, doi:10.5194/acp-11-6911-2011, 2011.

Xu, L., Suresh, S., Guo, H., Weber, R. J., and Ng, N. L.: Aerosol characterization over the southeastern United States using high-resolution aerosol mass spectrometry: spatial and seasonal variation of aerosol composition and sources with a focus on organic nitrates, Atmos. Chem. Phys., 15, 7307-7336, doi:10.5194/acp-15-7307-2015, 2015.

Xu, J., Zhang, Q., Chen, M., Ge, X., Ren, J., and Qin, D.: Chemical composition, sources, and processes of urban aerosols during summertime in northwest China: insights from high-resolution aerosol mass spectrometry, Atmos. Chem. Phys., 14, 12593-12611, doi:10.5194/acp-14-12593-2014, 2014.

Xu, J., Shi, J., Zhang, Q., Ge, X., Canonaco, F., Prévôt, A. S. H., Vonwiller, M., Szidat, S., Ge, J., Ma, J., An, Y., Kang, S., and Qin, D.: Wintertime organic and inorganic aerosols in Lanzhou, China: sources, processes, and comparison with the results during summer, Atmos. Chem. Phys., 16, 14937-14957, doi:10.5194/acp-16-14937-2016, 2016.

Xu, J., Zhang, Q., Shi, J., Ge, X., Xie, C., Wang, J., Kang, S., Zhang, R., and Wang, Y.: Chemical characteristics of submicron particles at the central Tibet Plateau: influence of long-range transport, Atmos. Chem. Phys. Discuss., 1-32, doi:10.5194/acp-2017-587, 2017.

Yao, T., Huang, X., He, L., Hu, M., Sun, T., Xue, L., Lin, Y., Zeng, L., and Zhang, Y.: High time resolution observation and statistical analysis of atmospheric light extinction properties and the chemical speciation of fine particulates, Sci. China Chem., 53, 1801-1808, doi:10.1007/s11426-010-4006-z, 2010.

Zhang, J. K., Sun, Y., Liu, Z. R., Ji, D. S., Hu, B., Liu, Q., and Wang, Y. S.: Characterization of submicron aerosols during a month of serious pollution in Beijing, 2013, Atmos. Chem. Phys., 14, 2887-2903, doi:doi:10.5194/acp-14-2887-2014, 2014a.

Zhang, L., Sun, J. Y., Shen, X. J., Zhang, Y. M., Che, H., Ma, Q. L., Zhang, Y. W., Zhang, X. Y., and Ogren, J. A.: Observations of relative humidity effects on aerosol light scattering in the Yangtze River Delta of China, Atmos. Chem. Phys., 15, 8439-

8454, doi:10.5194/acp-15-8439-2015, 2015a.

Zhang, Q., Jimenez, J. L., Canagaratna, M. R., Allan, J. D., Coe, H., Ulbrich, I., Alfarra, M. R., Takami, A., Middlebrook, A. M., Sun, Y. L., Dzepina, K., Dunlea, E., Docherty, K., DeCarlo, P. F., Salcedo, D., Onasch, T., Jayne, J. T., Miyoshi, T., Shimono, A., Hatakeyama, S., Takegawa, N., Kondo, Y., Schneider, J., Drewnick, F., Borrmann, S., Weimer, S., Demerjian, K., Williams, P., Bower, K., Bahreini, R., Cottrell, L., Griffin, R. J., Rautiainen, J., Sun, J. Y., Zhang, Y. M., and Worsnop, D. R.: Ubiquity and dominance of oxygenated species in organic aerosols in anthropogenically-influenced Northern Hemisphere midlatitudes, Geophys. Res. Lett., 34, doi:10.1029/2007gl029979, 2007.

Zhang, Q., Meng, J., Quan, J., Gao, Y., Zhao, D., Chen, P., and He, H.: Impact of aerosol composition on cloud condensation nuclei activity, Atmos. Chem. Phys., 12, 3783-3790, doi:10.5194/acp-12-3783-2012, 2012.

Zhang, X., Zhang, Y., Sun, J., Yu, Y., Canonaco, F., Prevot, A. S., and Li, G.: Chemical characterization of submicron aerosol particles during wintertime in a northwest city of China using an Aerodyne aerosol mass spectrometry, Environ. Pollut., doi:10.1016/j.envpol.2016.11.012, 2017.

Zhang, Y. J., Tang, L. L., Wang, Z., Yu, H. X., Sun, Y. L., Liu, D., Qin, W., Canonaco, F., Prévôt, A. S. H., Zhang, H. L., and Zhou, H. C.: Insights into characteristics, sources, and evolution of submicron aerosols during harvest seasons in the Yangtze River delta region, China, Atmos. Chem. Phys., 15, 1331-1349, doi:10.5194/acp-15-1331-2015, 2015b.

Zhang, Y. M., Zhang, X. Y., Sun, J. Y., Hu, G. Y., Shen, X. J., Wang, Y. Q., Wang, T. T., Wang, D. Z., and Zhao, Y.: Chemical composition and mass size distribution of PM_1 at an elevated site in central east China, Atmos. Chem. Phys., 14, 12237-12249, doi:10.5194/acp-14-12237-2014, 2014b.

Zhang, Y. W., Zhang, X. Y., Zhang, Y. M., Shen, X. J., Sun, J. Y., Ma, Q. L., Yu, X. M., Zhu, J. L., Zhang, L., and Che, H. C.: Significant concentration changes of chemical components of PM1 in the Yangtze River Delta area of China and the implications for the formation mechanism of heavy haze-fog pollution, Sci. Total. Environ., 538, 7-15, doi:10.1016/j.scitotenv.2015.06.104, 2015c.

Zheng, J., Hu, M., Du, Z., Shang, D., Gong, Z., Qin, Y., Fang, J., Gu, F., Li, M., Peng, J., Li, J., Zhang, Y., Huang, X., He, L., Wu, Y., and Guo, S.: Influence of biomass burning from South Asia at a high-altitude mountain receptor site in China, Atmos. Chem. Phys., 17, 6853-6864, doi:10.5194/acp-17-6853-2017, 2017.

Zhou, S., Collier, S., Jaffe, D. A., Briggs, N. L., Hee, J., Sedlacek Iii, A. J., Kleinman, L., Onasch, T. B., and Zhang, Q.: Regional influence of wildfires on aerosol chemistry in the western US and insights into atmospheric aging of biomass burning organic aerosol, Atmos. Chem. Phys., 17, 2477-2493, doi:10.5194/acp-17-2477-2017, 2017.

Zhu, Q., He, L. Y., Huang, X. F., Cao, L. M., Gong, Z. H., Wang, C., Zhuang, X., and Hu, M.: Atmospheric aerosol compositions and sources at two national background sites in northern and southern China, Atmos. Chem. Phys., 16, 10283-10297, doi:10.5194/acp-16-10283-2016, 2016.